Dual-Polarized Transmitarray with Independent Beam Control at K_a Band

Christos Exadaktylos, Abdul-Sattar Kaddour, and Stavros V. Georgakopoulos
Department of Electrical and Computer Engineering,
Florida International University
Miami, Florida, 33199, United States
cexad001@fiu.edu, akaddour@fiu.edu, georgako@fiu.edu

2022 IEEE International Symposium on Phased Array Systems & Technology (PAST) | 978-1-6654-4166-7/22/$31.00 ©2022 IEEE | DOI: 10.1109/PAST49659.2022.9975082

***Abstract*—This paper presents a five-layer, dual-polarized transmitarray antenna (TA) with independent beam control, operating at K_a Band (29 GHz) for point to point wireless communications. The proposed 5.2×5.2 mm² unit-cell is based on three rectangular strips on the receiving and transmitting layers for each polarization, which are connected using metalized vias. Each set of the three rectangular strips is designed to achieve a 180° phase resolution (i.e., 1-bit phase quantization) at the center frequency of our operating band. The proposed radiating element can form independent orthogonally polarized beams at the center frequency using the same radiating aperture. This TA design provides a maximum gain of 24.3 and 23.1 dBi at 0° and 20° scanning of the beam, respectively.**

***Index Terms*—Dual polarization, K_a band, high gain array, transmitarray (TA) antenna**

I. Introduction

Transmitarray antennas (TAs) are emerging as a promising solution for point to point wireless communications due to their advantageous features. Specifically, TAs provide planar designs, which are low-profile, lightweight, low-cost and easy to fabricate [1]. In addition, TAs exhibit no feed blockage (in contrast to reflectarrays that suffer from feed blockage), and provide high gain beam scanning in active configurations [2], [3]. Most beam-scanning TAs are designed for single polarized operation [4], [5]. However, simultaneous and independent dual-polarized operation is needed to achieve dynamic spatial coverage (scanning of the dual-polarized beams in different directions), or double the capacity of the channel (dual-polarized beams pointing in the same direction). To date, several dual-polarized TAs have been reported [6], [7], [8]. They usually suffer from complicated element designs, dependent beam synthesis, and difficulties in the implementation of electronically controlled beam scanning.

In this paper, a five-layer, dual-polarized high gain TA, which can achieve two independent orthogonally polarized beams at 29 GHz, is presented. The proposed unit-cell is based on two orthogonal radiating elements. Each radiating element consists of three narrowband patch elements (rectangular strips). Therefore, our design presents a TA unit-cell that supports both the horizontal and vertical polarization (H- and V-pol), while maintaining an overall size that is smaller than a half wavelength. This paper is organized as follows. Section II presents the unit-cell design, and its performance. Section III shows the full-wave simulation analysis of our design. Finally, Section IV discusses our conclusions.

This work was supported by the National Science Foundation under grant ECCS 2127762 and the Air Force Office of Scientific Research under grant FA9550-19-1-0290.

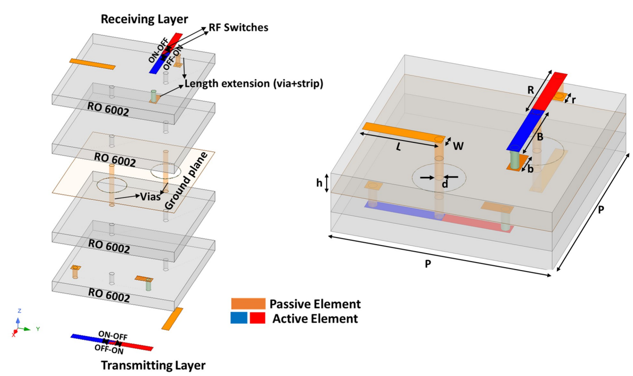

Fig. 1. Proposed 1-bit dual-pol TA unit-cell.

TABLE I
Geometry Parameters of the Proposed TA Unit-Cell

Symbol	Value (mm)	Symbol	Value (mm)
P	5.2	*W*	0.3
L	1.85	*d*	0.2
B	1.8	*b*	0.68
R	1.8	*r*	0.34

II. Dual-Polarized TA Unit-Cell Design

A. *Unit-cell Design*

The proposed TA unit-cell is presented in Fig. 1. Its overall size is 5.2×5.2 mm² (which is equivalent to $0.5\lambda\times0.5\lambda$, where λ is the wavelengths at 29 GHz). Such a small lattice size allows beam scanning over a wide field of view, both in the H- and V-pol beams (H-pol being along the x-axis and V-pol being along the y-axis). In this design, two rectangular strips are used in the receiving layer, and one rectangular strip is used in the transmitting layer for the H-pol. The configuration is reversed for the V-pol, which means that one rectangular strip is placed in the receiving layer, and two rectangular strips are placed in the transmitting layer. These strips are printed on 0.508-mm-thick Rogers RT/Duroid 6002 substrates (ϵ_r = 2.94, tanγ = 0.0012), and are linearly-polarized along the x- and y-axis. The respective receiving and transmitting elements for the H- and V-pol are connected through metalized vias. A metallic ground plane with two circular holes is placed between the receiving and transmitting elements. Two RF switches, indicated as SH_1 and SH_2 are placed on the H-pol receiving element, as shown in Fig. 1, respectively. Also, two RF switches, indicated as SV_1 and SV_2 are placed on the V-pol transmitting element. With such configuration, we can electronically control the transmission phase of the unit-cell simultaneously and independently with a 1-bit phase resolution for the H-pol and the V-pol. For simplification, in this design, the RF switches in the ON and OFF states are replaced by short and open stubs, respectively. The geometrical parameters of our unit cell are shown in Table I.

B. Operation Principle

For each radiating element, the corresponding RF switches operate in opposite states (one switch is in ON state while the other is in OFF state, and vice versa). Switching between these two states leads to opposite surface currents on the receive element and transmit element for the H- and V-pol, as shown in Fig. 2. Thus a 180° phase-shift is achieved between the receiving element and transmitting elements for the H- and V-pol. These different unit-cell phase states are called H_0V_0, H_0V_{180}, $H_{180}V_0$ and $H_{180}V_{180}$. Table II presents the four UC states. Additionally, the RF switch-loaded elements (active elements) are asymmetrically extended with the use of a via and a strip. This feature of the design accounts for the asymmetric coupling between the active and passive element, and ensures that the active element resonates at the same frequency (29 GHz) no matter the state of the RF switches and for both polarizations.

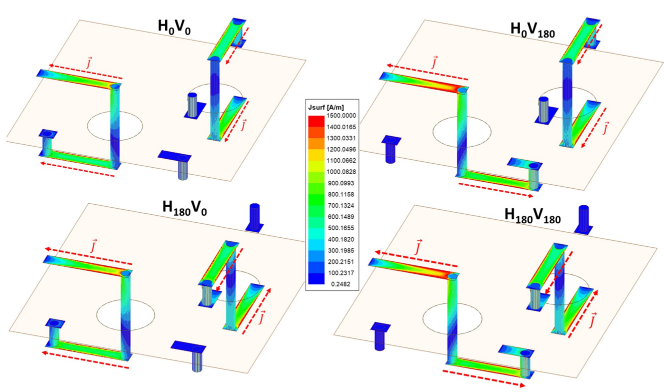

Fig. 2. Surface current distributions of the unit cell for the four phase states of our radiating elements and for H-, V-pol, respectively.

C. Performance of the Dual-Polarized TA Unit Cell

The proposed unit cell was simulated in ANSYS HFSS. Periodic boundary conditions and Floquet ports excitation were used to consider the mutual coupling between surrounding unit-cells. The scattering parameters of our proposed unit cell are shown at its four different states in Fig. 3. Notably, only normal incidence is considered here. It is seen that the insertion loss is lower than 0.21 dB and 0.41 dB for the in and out of phase transmissions, respectively (for both polarizations). Also, Fig. 3(c) shows that a 180° phase shift is achieved (1-bit of phase resolution) over the entire band of interest for both polarizations. Therefore, the two orthogonally polarized beams of our TA unit cell can be independently controlled by the RF switches. The RF switch-loaded elements (active elements) are placed in opposite ends of the structure (H-pol active element in the receiving layer and V-pol active element in the transmitting element). This feature de-associates the two polarizations, and is expected to result in lower losses and easier fabrication of the equivalent active TA (PIN diodes and a dc bias control circuit will be used to dynamically steer the two beams).

TABLE II
PROPOSED UNIT CELL STATES

UC state	SH_1	SH_2	SV_1	SV_2	$\angle T_H$(°)	$\angle T_V$(°)
H_0V_0	OFF	ON	ON	OFF	0	0
H_0V_{180}	OFF	ON	OFF	ON	0	180
$H_{180}V_0$	ON	OFF	ON	OFF	180	0
$H_{180}V_{180}$	ON	OFF	OFF	ON	180	180

III. DUAL-POLARIZED TRANSMITARRAY WITH INDEPENDENT BEAM CONTROL

The 1-bit dual-polarized unit-cell presented in Section II is used here to design a 20×20 high-gain transmitarray. A dual-polarized pyramidal horn is used to illuminate the TA, and is placed at a distance F = 90 mm from the array aperture (i.e., F/D = 0.87). This feed's gain is 15.4 dBi at 29 GHz. The focal distance and the phase distributions were chosen to maximize our TA's gain and aperture efficiency (illumination and spillover) for both the H- and V-pol. Fig. 4 shows the dual-polarized TA design with its horn feed. The radiation patterns of the proposed TA are computed through full-wave simulations in ANSYS HFSS.

Two different 20×20 TAs were designed TA-I and TA-II. TA-I was designed to independently point its H-pol and V-pol beams at 0° and 20° off broadside (in the H-pol plane i.e. xz plane), respectively. Whereas, TA-II was designed to independently steer its H-pol and V-pol beams at -20° and 20° off broadside (in the H-pol plane i.e. xz plane), respectively. Thus, the V-pol beam points in the the same direction, while the H-pol beam is steered in two different directions for the two TAs. In this manner, we showcase the independent control of the two polarizations. The TA-I and TA-II 1-bit phase distributions that are required to independently steer the beams towards the desired directions are calculated for both polarizations, and they are plotted in Fig. 5. The normalized gain patterns computed for both TA-I and TA-II and for both polarizations are represented in Fig. 6, respectively. The results of Fig. 6 show that the H-pol beam is indeed scanned. The V-pol beam points in the same direction unaffected by the

978-1-6654-4166-7/22/$31.00 ©2022 IEEE

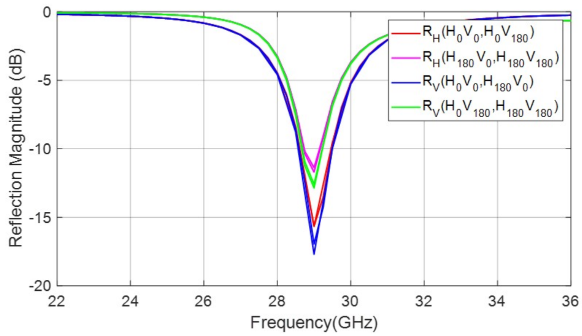

(a)

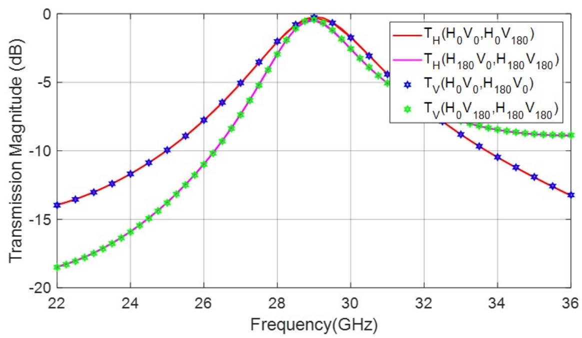

(b)

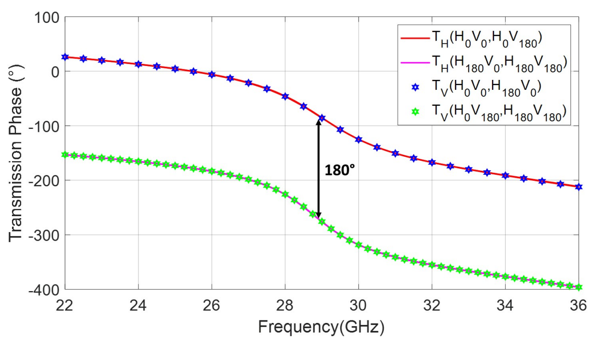

(c)

Fig. 3. Scattering parameters of proposed unit cell at its different operating states (a) Reflection Magnitude, (b) Transmission Magnitude and, (c) Transmission Phase.

scanning of the H-pol beam. Thus, independent control of the two orthogonally polarized beams is demonstrated. Also, the V-pol beam (20° off broadside for TA-I and TA-II) achieves 23.1dBi of gain. The H-pol beam (0 and -20° off broadside for TA-I and TA-II respectively) achieves a gain of 24.3 and 23.2dBi, thereby exhibiting only 1.1dB of scan loss.

IV. Conclusion

We presented a dual polarized (DP) high-gain transmitarray that can independently steer its beams toward different directions for the two polarizations, H-pol and V-pol. A 1-bit phase resolution is achieved for both polarizations by changing the states of two RF switches on each radiating element. Also, since our TA uses only four PCB layers, it has lower cost and smaller weight than previously reported designs. Therefore, the proposed dual-pol transmitarray antenna is very well-suited for point to point wireless communications and radar systems.

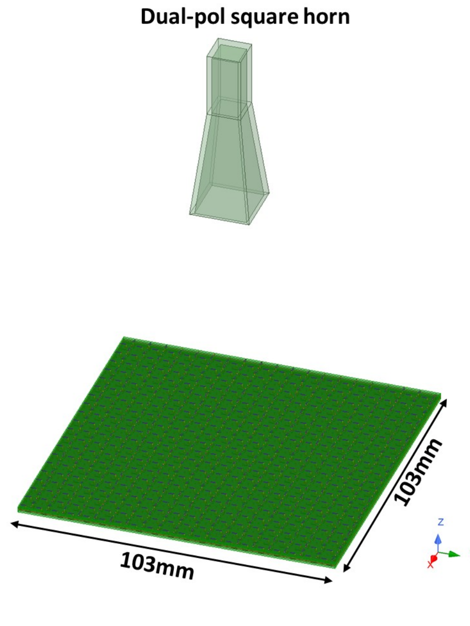

Fig. 4. Proposed transmitarray antenna.

Acknowledgment

This work was supported by the National Science Foundation under grant ECCS 2127762 and the Air Force Office of Scientific Research under grant FA9550-19-1-0290.

References

[1] K. T. Pham, A. Clemente, E. Fourn, F. Diaby, L. Dussopt and R. Sauleau, "Low-Cost Metal-Only Transmitarray Antennas at Ka-Band," in IEEE Antennas and Wireless Propagation Letters, vol. 18, no. 6, pp. 1243-1247, June 2019, doi: 10.1109/LAWP.2019.2913571.

[2] Y. Wang, S. Xu, F. Yang and D. H. Werner, "1 Bit Dual-Linear Polarized Reconfigurable Transmitarray Antenna Using Asymmetric Dipole Elements With Parasitic Bypass Dipoles," in IEEE Transactions on Antennas and Propagation, vol. 69, no. 2, pp. 1188-1192, Feb. 2021, doi: 10.1109/TAP.2020.3005713.

[3] X. Dai, G. -B. Wu and K. -M. Luk, "A Wideband Low-Profile Reconfigurable Transmitarray Using Magnetoelectric Dipole Elements," in IEEE Transactions on Antennas and Propagation, doi: 10.1109/TAP.2022.3164185.

[4] Y. Wang, S. Xu, F. Yang and M. Li, "A Novel 1 Bit Wide-Angle Beam Scanning Reconfigurable Transmitarray Antenna Using an Equivalent Magnetic Dipole Element," in IEEE Transactions on Antennas and Propagation, vol. 68, no. 7, pp. 5691-5695, July 2020, doi: 10.1109/TAP.2020.2964954.

[5] A. Clemente, L. Dussopt, R. Sauleau, P. Potier and P. Pouliguen, "Wideband 400-Element Electronically Reconfigurable Transmitarray in X Band," in IEEE Transactions on Antennas and Propagation, vol. 61, no. 10, pp. 5017-5027, Oct. 2013, doi: 10.1109/TAP.2013.2271493.

[6] F. Wu, J. Wang, L. Xiang, W. Hong and K. -M. Luk, "A Wideband Dual-Polarized Magneto-Electric Dipole Transmitarray with Independent Control of Polarizations," in IEEE Transactions on Antennas and Propagation, doi: 10.1109/TAP.2022.3168678.

[7] K. T. Pham, R. Sauleau, E. Fourn, F. Diaby, A. Clemente and L. Dussopt, "Dual-Band Transmitarrays With Dual-Linear Polarization at Ka-Band," in IEEE Transactions on Antennas and Propagation, vol. 65, no. 12, pp. 7009-7018, Dec. 2017, doi: 10.1109/TAP.2017.2762011.

978-1-6654-4166-7/22/$31.00 ©2022 IEEE

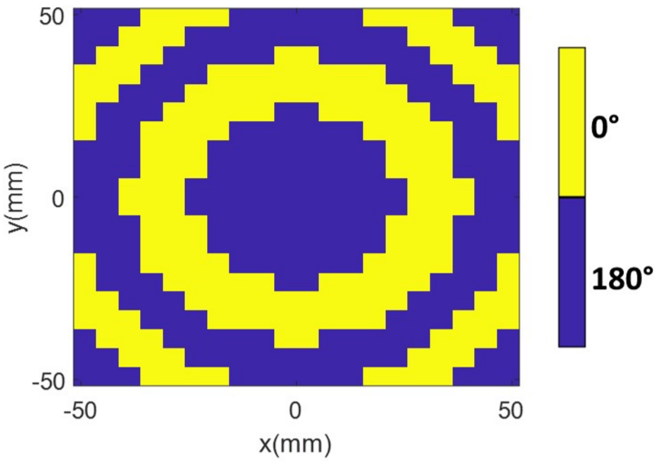

(a)

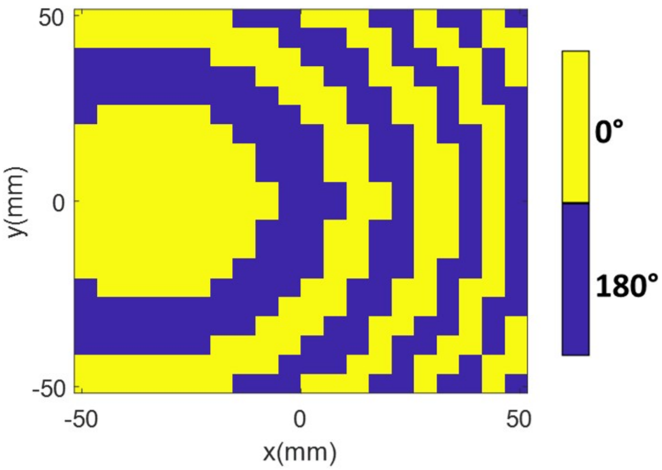

(b)

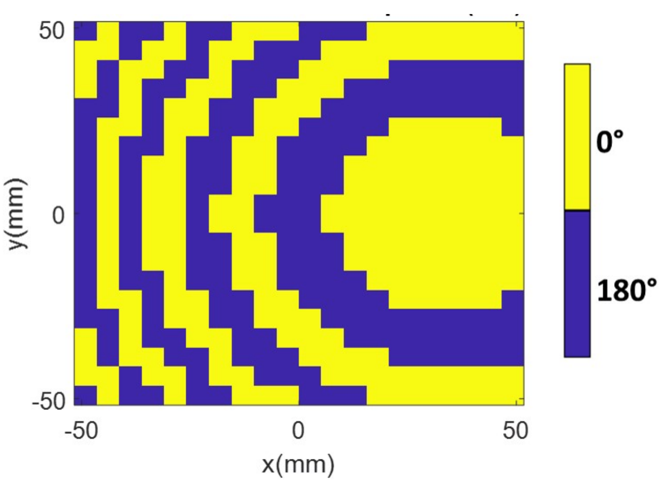

(c)

Fig. 5. Transmisson phase distributions for (a) TA-I, H-pol, (b) TA-II, H-pol and (c) TA-I and TA-II, V-pol.

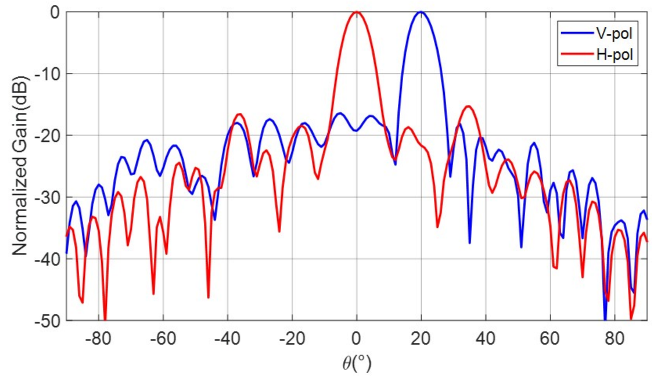

(a)

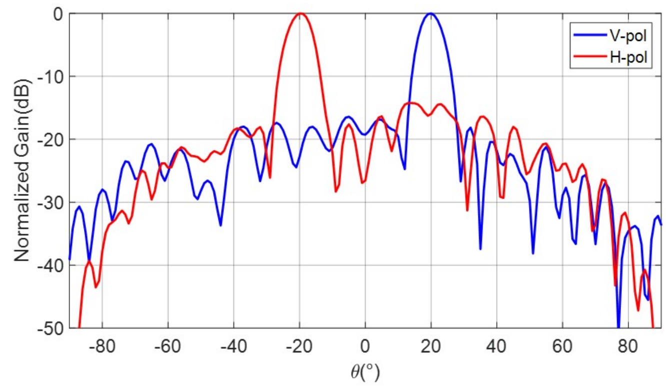

(b)

Fig. 6. Normalized gain radiation patterns in the xz-plane i.e. H-pol plane for (a) TA-I and (b) TA-II.

[8] R. Madi, A. Clemente and R. Sauleau, "Dual-Band, Dual-Linearly Polarized Transmitarrays for SATCOM Applications at Ka-Band," 2022 16th European Conference on Antennas and Propagation (EuCAP), 2022, pp. 1-4, doi: 10.23919/EuCAP53622.2022.9768892.

978-1-6654-4166-7/22/$31.00 ©2022 IEEE